Yongke Yan*, Anthony Marin, Yuan Zhou and Shashank Priya*

# Enhanced Vibration Energy Harvesting Through Multilayer Textured $Pb(Mg_{1/3}Nb_{2/3})O_3$–$PbZrO_3$–$PbTiO_3$ Piezoelectric Ceramics

**Abstract:** High-performance low-cost multilayer textured $Pb(Mg_{1/3}Nb_{2/3})O_3$–$PbZrO_3$–$PbTiO_3$ (PMN–PZT) piezoelectric ceramic benders were fabricated by combining templated grain growth (TGG) and low-temperature co-firing ceramics (LTCC) process. The $d \times g$ values of textured samples were 700–800% higher than that of the random counterpart, which results in 500–600% increase in the output power from vibration energy harvesting. The output power and power density of tri-layer textured sample at the acceleration of 0.43 g were measured to be 903 μW and 15.5 $mW/cm^3$, respectively. The results demonstrate that the multilayer structure results in an increase in output current and a decrease in the matching resistive load.

**Keywords:** piezoelectric, textured ceramics, multilayer, co-firing, energy harvesting

DOI 10.1515/ehs-2014-0001

Self-powered wireless sensor nodes are being demanded for multiple applications ranging from personal healthcare to building efficiency. Variety of low-power solutions are being explored globally to meet this rising demand ranging from high-efficiency solar cells to thermal energy harvesters to mechanical energy harvesters (Dondi et al. 2008; Leonov et al. 2007; Roundy and Wright 2004). Each of these solutions holds promise in a given scenario as one source of energy may not be available across all the platforms. Mechanical energy harvesting has been mainly investigated for meeting the extremely low-power sensing needs ranging from μW to mW and there is continuous ongoing effort in improving their power density. Mechanical energy can be converted into electrical energy through various possible mechanisms including piezoelectric, electromagnetic, electrets, electrostatic, dielectric elastomers, and so on (Roundy and Wright 2004; Mitcheson et al. 2008; Khaligh, Zeng, and Zheng 2010; Kambale et al. 2014; Apo, Sanghadasa, and Priya 2014; Burghardt et al. 2014). Piezoelectrics are attractive at smaller dimensions and where magnetic fields are of concern. In this letter, we demonstrate that power density of piezoelectric energy harvester for capturing ambient mechanical vibration energy can be significantly improved by tailoring the magnitude of electromechanical parameters through grain texturing.

The primary factor for the selection of piezoelectric materials is the transduction rate whose magnitude is governed by the product of piezoelectric strain constant, $d$, and the effective piezoelectric voltage constant, $g$ since electric energy available under an alternating stress excitation is given by Priya (2010); Islam and Priya (2006):

$$P = U_e = \frac{1}{2}CV^2 = \frac{1}{2}\varepsilon_0\varepsilon_r\frac{A}{t}\left(-\frac{g \times F \times t}{A}\right)^2 = \frac{1}{2}(d \times g) \times \left(\frac{F}{A}\right)^2 \times (At) \quad [1]$$

or energy density ($u_e$),

$$u_e = \frac{1}{2}(d \times g) \times \left(\frac{F}{A}\right)^2 \quad [2]$$

where $F$ is the applied force, $A$ is the area, and $t$ is the thickness of active piezoelectric material. Equation [2] shows that under given experimental conditions, a material with high $(d \times g)$ product will generate higher power. However, there is challenge in achieving high $d \times g$

***Corresponding author: Yongke Yan,** Bio-inspired Materials and Devices Laboratory (BMDL), Center for Energy Harvesting Materials and Systems (CEHMS), 310 Durham Hall, Virginia Tech, Blacksburg, VA 24061, USA, E-mail: yanthu@gmail.com
**Shashank Priya,** Bio-inspired Materials and Devices Laboratory (BMDL), Center for Energy Harvesting Materials and Systems (CEHMS), 310 Durham Hall, Virginia Tech, Blacksburg, VA 24061, USA, E-mail: spriya@vt.edu
**Anthony Marin:** E-mail: marinvt@gmail.com, **Yuan Zhou:** E-mail: yzhou6@vt.edu, Bio-inspired Materials and Devices Laboratory (BMDL), Center for Energy Harvesting Materials and Systems (CEHMS), 310 Durham Hall, Virginia Tech, Blacksburg, VA 24061, USA

coefficient via the composition modification in conventional piezoelectric ceramic because any increase in the piezoelectric constant ($d$) is always accompanied by the large increase in dielectric susceptibility ($\varepsilon$), thus, high $d$ usually shows low $g$. Recently, we found that templated grain growth (TGG) technique yields textured relaxor-PT/PZT piezoelectric ceramics with large ($d \times g$) magnitude (Yan et al., 2013; Yan, Wang, and Priya 2012). Using this technique, we achieved two goals: (1) <001> texturing (grain orientation along the <001> crystallographic direction) of piezoelectric ceramic with engineered domain state to achieve high $d$ and (2) realization of high $d \times g$ coefficient by suppressing $\varepsilon$ of textured piezoelectric ceramic through the use of low $\varepsilon$ templates (Yan et al. 2013).

As a power source, the piezoelectric material can generate a very large voltage but at low current amplitude. When charging a battery or supercapacitor, a larger current is needed to shorten the charging time. Further, the matching impedance for piezoelectrics is on the order of ~1 MΩ while sensor nodes have impedance on the order of 100 Ω; thus, complex impedance matching circuits are needed to optimize the power cycle (Kong et al. 2010). The capacitance and output charge of multilayer capacitor can be dramatically increased with the number of layers, thereby, tune the electric characteristics as piezoelectric energy harvester as shown below (Roundy and Wright 2004; Zhu et al. 2010)

$$C_n = \varepsilon_0 \varepsilon_r \frac{A}{t/n} \times n = n^2 \times C;$$

$$V_{\text{open}} = E \times t = -g \times X \times t = -\frac{g \times F \times t}{A};$$

$$R_{\text{match}} = \frac{1}{2\pi f C} \times \frac{2\zeta}{\sqrt{4\zeta^2 + k^4}};$$

$$R_{\text{match},n} = \frac{1}{n^2} \times R_{\text{match}}; V_{\text{open},n} = \frac{1}{n} \times V_{\text{open}}; I_n = n \times I; P_n = P \quad [3]$$

where $C$, $R_{\text{match}}$, $I$ and $V_{\text{open}}$ are capacitance, matching resistance, current and open voltage of single layer structure, respectively; $C_n$, $R_{\text{match},n}$, $I_n$ and $V_{\text{open},n}$ are capacitance, matching resistance, current and open voltage of $n$ layer structure, respectively; $f$ is operating frequency, $\zeta$ and $k$ are damping ratio and piezoelectric coupling coefficient, respectively, and $X$ is stress applied on the piezoelectric materials. It can be seen that through multilayer structure, the matching resistance and voltage can be decreased and the current can be increased to meet the requirement for sensing node. By combining eqs [2] and [3], we can anticipate that improvement in piezoelectric material properties along with multilayer structure will result in higher power along with optimum magnitude of matching impedance.

To fabricate the multilayer ceramics, a proven and cost-effective methodology is by using low-temperature co-fired ceramics (LTCC) process. This process has been widely used for synthesis of multilayer ceramic capacitor (MLCC) and multilayer actuator (MLA) (Gongora-Rubio et al. 2001). In this study, we successfully combined TGG process with LTCC process to create high-performance low-cost multilayer textured piezoelectric bender. The $d \times g$ values of textured samples were about 700–800% higher than that of the random counterpart, which results in 500–600% increase in output power from vibration energy harvesting. The multilayer structure results in an increased output current and a decreased matching resistive load.

Figure 1 shows the schematic diagram of co-fired multilayer textured ceramics based on TGG process and LTCC process. The composition 0.4Pb $(Mg_{1/3}Nb_{2/3})O_3$–$0.25PbZrO_3$–$0.35PbTiO_3$ (PMN–PZT) was chosen as matrix, and $BaTiO_3$ (BT) platelets were used as template for texturing PMN–PZT. PMN–PZT precursor powder was synthesized by conventional solid state reaction. Mixture of $2PbCO_3 \cdot Pb(OH)_2$ (99.9%, Sigma Aldrich, St. Louis, MO), $MgNb_2O_6$ (99.9%, Alfa Aesar, Ward Hill, MA), $ZrO_2$ (30–60 nm, Advanced Materials LLC, Manchester, CT), $TiO_2$ (~40 nm, Advanced Materials LLC) was ball-milled in ethanol for 48 h using $ZrO_2$ (Tosoh USA, Grove City, OH) ball-milling media. After drying, the mixture was calcined at 750°C for 2 h. The calcined powder was then ball-milled with 1 wt% PbO (99.9%, Sigma Aldrich, St. Louis, MO) for 48 h. After drying, the powder was sieved through 170 mesh sieve. The templates were synthesized by topochemical microcrystal conversion method (Liu, Yan, and Zhou 2007). The BT template microcrystals were aligned in PMN–PZT green ceramic tape-by-tape casting as described in details elsewhere (Yan et al. 2013). Then the silver paste (9770, DuPont, NC, USA) was screen-printed on the textured PMN–PZT green tape for inner electrodes. At last the printed tapes were cut, stacked, laminated, and then co-fired at 800–950°C for 2 h in the air. The final samples possess the textured microstructure and multilayer structure as illustrated in Figure 1. Random PMN–PZT samples were also prepared for comparative analysis by the same procedure without adding BT template. The crystal structure and microstructure of textured PMN–PZT ceramics were determined using X-ray diffraction (XRD, PANalytical X'Pert, CuKα) and scanning electron microscope (SEM, FEI Quanta 600 FEG), respectively. The degree of pseudocubic <001> texture was determined by Lotgering factor method from XRD on polished sample surfaces parallel to the tape-casting plane. The capacitance of poled samples was

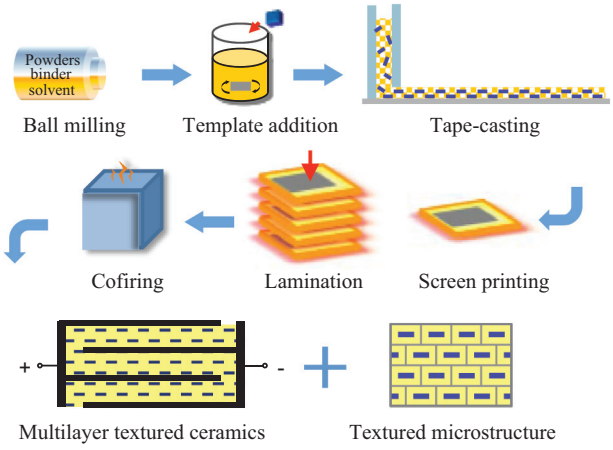


**Figure 1** Schematic diagram of co-fired multilayer textured ceramics based on TGG process and LTCC process

measured by using a multi-frequency LCR meter (HP7274A). The strain as a function of electric field was measured by using a modified Sawyer-Tower circuit (Precision Premier II, Radiant Technologies Inc.) combined with a linear variable differential transducer (LVDT) driven by a lock-in amplifier (model SR830, Stanford Research Systems). For vibration energy harvesting measurement, co-fired multilayer textured piezoelectric benders were attached on the stainless steel stripes by epoxy. These cantilevers were then mounted on a LDS shaker (Bruel & Kjaer North America, Inc.) using a custom clamp and excited by a sinusoidal sweep. A tip mass (1.1 g) was attached at the free end of cantilever for dynamic force excitation at the mechanical resonance. The base acceleration was measured by a low mass accelerometer (PCB U352C22) and the velocity response of the harvester at the free end was measured by laser vibrometer (PDV 100, Polytech, Inc.). All the signals were collected by using Siglab analyzer (Model 20-42) through the process described in detail elsewhere (Bedekar, Oliver, and Priya 2010).

Co-firing temperature should be lower than the melting point of Ag (961°C) for using Ag electrode, while the texture development requires higher sintering temperature as it is nucleation and growth-driven process (Messing et al. 2004; Sabolsky, Messing, and Trolier-McKinstry 2001; Tani and Kimura 2006) Possible low-temperature sintering induced defects (such as porosity, poor mechanical adhesion, and electrical contact of piezoelectric–electrode interface) could degrade piezoelectric properties. Therefore, there is a trade-off between electrode composition and texture degree. Figure 2(a) shows the cross-sectional SEM images of fractured textured ceramics co-fired at different temperatures. BT templates (black lines) were found to be well aligned in the matrix. The matrix particles started to nucleate and grow from the BT template around 800°C. The growth distance for the sample co-fired at 850°C rapidly increased to about 5 μm and most of matrix particles were consumed at the temperature of 900°C. Further increase in the sintering temperature to 925°C resulted in only slight increase in the texture. The samples exhibited high density (>96%) above sintering temperatue of 900°C. The good sinterability of textured PMN–PZT is due to the fine grain particles (100–200 nm) and the addition of PbO liquid sintering aid. The liquid phase promotes the sintering and texture formation because mass transport

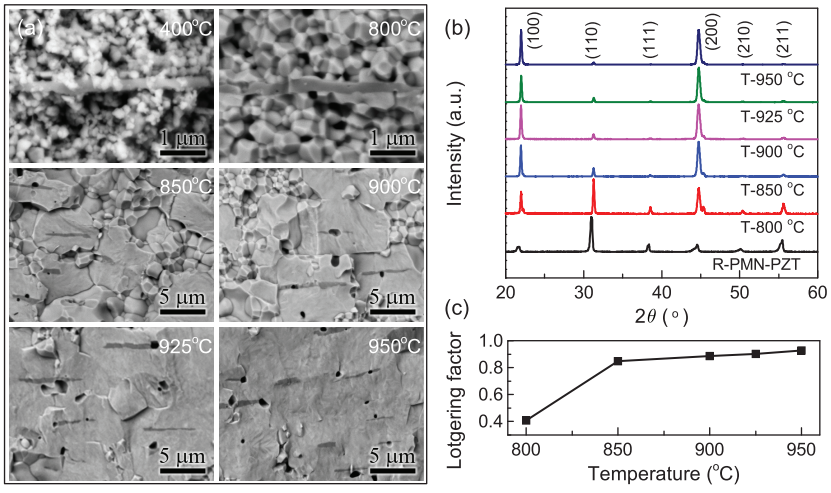


**Figure 2** (a) Cross-sectional SEM images of textured ceramics (fracture) co-fired at different temperatures. (b) XRD patterns of random ceramics (R-PMN–PZT) and textured ceramics (T) co-fired at different temperatures. (c) Lotgering factors of textured ceramics co-fired at different temperatures

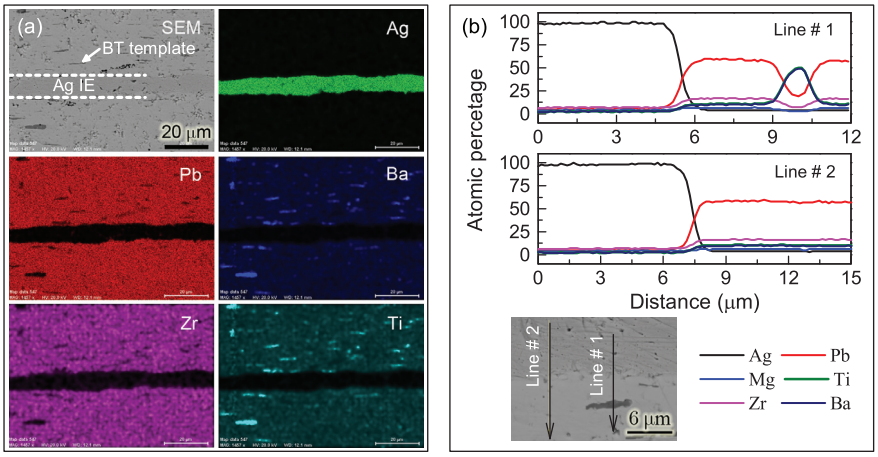


**Figure 3** (a) SEM images and EDS element mapping and (b) line scan element analysis of co-fired textured PMN–PZT ceramics sintered at 925°C for 2 h (polished cross-section)

in liquid phase is much faster than diffusion in solid phase.

Texture development is strongly correlated with the microsturcture evolution. Figure 2(b) shows the XRD pattern of textured ceramics co-fired at different temperatures. All patterns display perovskite structure without pyrochlore phase. There was no other peaks corresponding to Ag or related compound, which indicates no detectable Ag migration and chemical reaction with PMN–PZT occurred under the selected sintering conditions. With increasing sintering temperature, the intensities of 00*l* peaks increased while other peak intensities decreased indicating the increase in texture degree. Figure 2(c) shows the texture degree evaluated by Lotgering factor as a function of co-firing temperature. The Lotgering factor increases rapidly from 800°C and saturates after 850°C. The samples co-fired at 925°C exhibited 90% texture degree.

Figure 3(a) shows the polished cross-sectional SEM images and EDS element mapping of textured ceramics co-fired at 925°C. The interface between textured PMN–PZT piezoelectric layer and Ag inner electrode exhibited good adhesion. EDS mapping of textured ceramic/Ag inner electrode co-fired at 925°C indicated that there is clear interface between the matrix and template, and no obvious interfacial reaction and diffusion was confirmed by line scanning analysis as shown in Figure 3(b). Figure 4 shows the strain behavior of tri-layer textured ceramic (T-3), single layer textured (T-1) and random ceramic (R-1) and single crystal. The strain vs electric field (*S-E*) plot shows linear behavior even under high field condition of 20 kV/cm (Figure 4(a)). The piezoelectric strain coefficients determined from the slope of *S-E* curve, resulted in $d_{33}$ (*S*/*E*, 20 kV/cm) values of 1,121 pm/V, 1,128 pm/V, and 408 pm/V for T-3, T-1, and R-1, respectively. The $d_{33}$ values of textured samples (T-1, T-3) were significant higher than the random sample (R-1) and are almost comparable to their single crystal (SC) counterpart (1,560 pm/V) (Zhang et al. 2008). From Figure 4(b), it can be observed that the driving voltage is required to achieve a certain magnitude of strain decreases in proportion to the number of layers. Table 1 lists the piezoelectric properties of random and textured samples with different layers. The piezoelectric properties of textured sample are significantly higher than the random counterpart. The high electromechanical coupling coefficients in textured sample were obtained due to the special crystallographic orientation of grains in textured ceramics (strong orientation along the radial poling

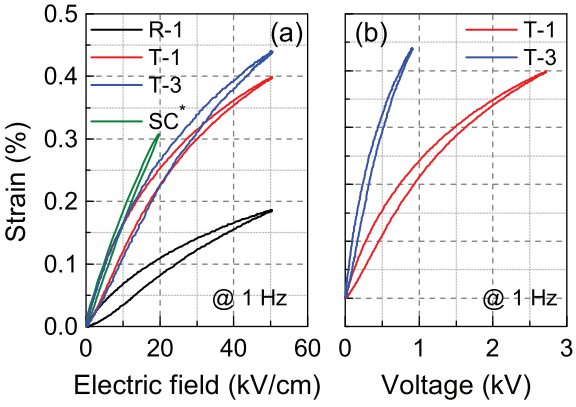


**Figure 4** (a) Strain vs electric field (*S-E*) curves for different PMN–PZT materials, tri-layer textured ceramic (T-3), single layer textured ceramic (T-1), random ceramic (R-1) and single crystal. (b) Strain vs driving voltage for textured ceramics: single layer (T-1) and tri-layer (T-3)

**Table 1** Piezoelectric properties measured by resonance/antiresonance method and energy harvesting properties of random single layer (R-1), textured single layer (T-1), bi-layer (T-2), and tri-layer (T-3) samples tested at the acceleration of 0.1 g

| Samples | $k_{31}$ | $d_{31}$* (pC/N) | $g_{31}$* ($10^{-3}$ Vm/N) | $d_{31}$* × $g_{31}$* ($10^{-15}$ m$^2$/N) | $R_{match}$ (kOhm) | $U$ (V) | $I$ (μA) | $P_{max}$ (μW) |
|---|---|---|---|---|---|---|---|---|
| R-1 | 0.27 | 78 | 9.6 | 749 | 600 | 3.83 | 6.4 | 24.4 |
| T-1 | 0.51 | 366 | 14.7 | 5,380 | 500 | 7.22 | 14.4 | 104.3 |
| T-2 | 0.52 | 780 | 7.3 | 5,694 | 120 | 3.92 | 32.7 | 128.1 |
| T-3 | 0.52 | 1,048 | 5.0 | 5,438 | 60 | 2.87 | 47.8 | 137.2 |

direction and random distribution in the plane) (Yan, Zhou, and Priya 2014). The $d \times g$ values of textured samples were about 800% higher than that of the random counterpart. The high $d \times g$ coefficient of textured samples was realized from: (1) high $d$ via <001> engineered domain configuration and (2) high $g$ via suppressing dielectric constant ($\varepsilon$) by using low $\varepsilon$ templates. It should be noted here that the intrinsic piezoelectric charge coefficient ($d$) and voltage coefficient of piezoelectric materials should be same regardless of one layer or multilayer. However, due to the change of the capacitance in the multilayer structure as described in eq. [3], the measured and calculated piezoelectric charge coefficient ($d$) in multilayer structured samples will increase by $n$ times and voltage coefficient ($g$) will decrease by $n$ time, while the $d \times g$ value will be same. In order to clarify the difference between the measured piezoelectric coefficients in the multilayer structures and the intrinsic piezoelectric coefficients in piezoelectric materials, the symbols $d$* and $g$* were used to represent the measured piezoelectric charge and voltage coefficients in Table 1, respectively.

Figure 5(a) shows the configuration of cantilever and the setup for vibration testing. The co-fired textured ceramics were about 38 mm in length (35 mm, effective), 7 mm in width, and 0.32 mm in thickness. For comparative study, the dimensions and test configurations for all the samples (R-1, T-1, T-2 and T-3) were kept same. Figure 5(b) depicts the frequency dependence of open circuit voltage. It shows that the resonance frequencies of all cantilevers were as low as 20 Hz, which is mainly dependent on the flexible stainless steel stripes. The open

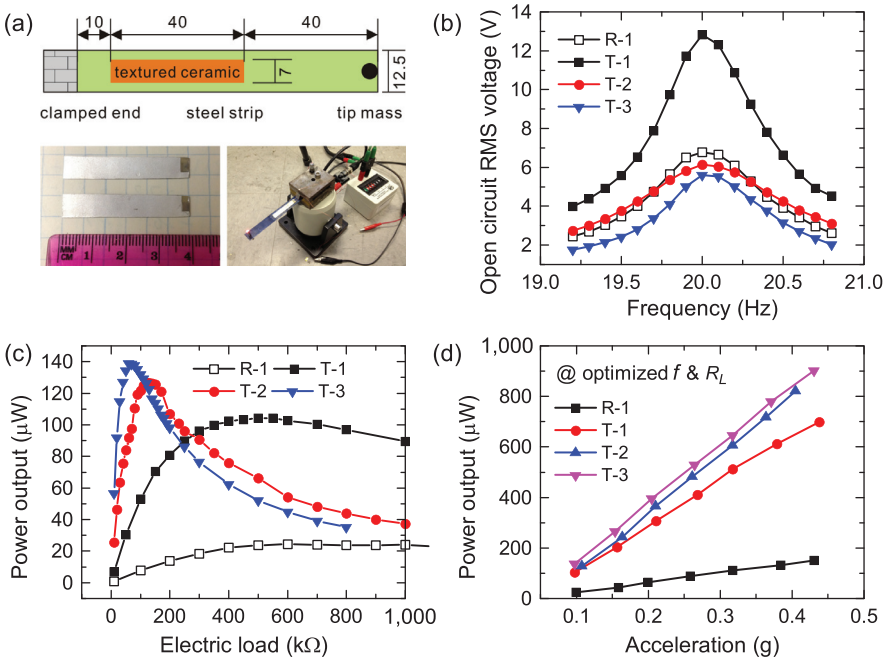


**Figure 5** (a) Schematic diagram of cantilever configuration (unit: mm), optical image of co-fired textured ceramics and the setup for vibration testing. (b) Open circuit voltage (RMS) as a function frequency; (c) Power as a function of resistive load. (d) Power output of single layer (T-1), bi-layer (T-2), tri-layer (T-3) and single layer random (R-1) samples tested at different acceleration (1 g = 9.8 m/s$^2$)

circuit voltage of single layer textured sample (T-1) was almost twice as that of single layer random sample (R-1). According to eq. [2], the generated voltage of piezoelectric ceramic is determined by piezoelectric voltage coefficient ($g$). As shown in Table 1, the $g$ for T-1 ($14.7 \times 10^{-3}$ Vm/N) is much higher than that of R-1 ($9.6 \times 10^{-3}$ Vm/N). For co-fired textured sample (T-1, T-2, and T-3), the generated voltage decreases with the increase in the number of layers (Figure 5(b)), and the optimum resistive load decreases with increase in number of layers (Figure 5(c)). In ideal condition, open circuit voltage of a $n$-layer generator will be $n$ times smaller than that of a single layer generator, and the optimum resistive load of a $n$-layer generator will be $n^2$ times smaller than that of a single layer generator which is consistent with the experiment results listed in Table 1. Figure 5(d) displays output power of all the samples as a function of acceleration. The output power and power density of T-3 sample at the acceleration of 0.43 g were found to be 903 μW and 15.5 mW/cm$^3$, respectively. The output power of co-fired multilayer textured samples was 500–600% higher than that of random sample. The output power of textured sample slightly increased with the number of layers. This trend is slightly different from the results reported by Zhu et al. (the double-layer generator produced slightly higher power than a single layer and tri-layer) (Zhu et al. 2010). However, it could be inferred that the variation in output power level of samples with different layers was within a small range which could be related to the interfaces and electrode effects. Further, the small variation could be attributed to the effects arising during sintering and epoxy bonding. Figure 6 compares the $d \times g$ value of textured ceramics with the available commercial piezoelectric ceramics. The $d \times g$ values of textured samples were significantly higher than those of commercial piezoelectric ceramics, and 700–800% higher than that of the random counterpart. Based on eq. [2], the high $d \times g$ values could be the reason of 500–600% increase in output power from the textured samples.

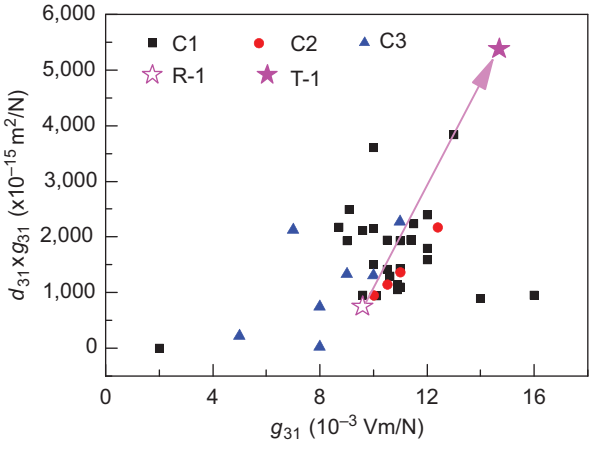


**Figure 6** Comparison of the magnitude of $d_{31} \times g_{31}$ as a function of $g_{31}$ for the random (R-1) and textured (T-1) samples in this study with commercially available ceramics

In summary, high-performance low-cost multilayer textured PMN–PZT piezoelectric ceramic benders were fabricated by combining TGG and LTCC process. The output power and power density of T-3 sample at the acceleration of 0.43 g were found to be 903 μW and 15.5 mW/cm$^3$, respectively. These results are highly promising for design of the power sources that can meet the sensor nodes in the requisite package.

**Acknowledgments:** The authors would like to thank the NSF I/UCRC: Center for Energy Harvesting Materials and Systems (CEHMS) for supporting the work on synthesis of textured piezoelectric materials. The authors also gratefully acknowledge the financial support from Office of Basic Energy Science, Department of Energy through grant # DE-FG02-07ER46480 (Y.Z.).

## References

Apo, D. J., M. Sanghadasa, and S. Priya. 2014. "Vibration Modeling of Arc-Based Cantilevers for Energy Harvesting Applications." *Energy Harvesting and Systems* 1:57.

Bedekar, V., J. Oliver, and S. Priya. 2010. "Design and Fabrication of Bimorph Transducer for Optimal Vibration Energy Harvesting." *IEEE Transactions on Ultrasonics Ferroelectrics and Frequency Control* 57(7):1513–23.

Burghardt, F. L., A. C. Waterbury, I. Paprotny, L. M. Miller, P. Minor, R. Send, Q. Xu, R. M. White, and P. K. Wright. 2014. "A Design Methodology for Energy Harvesting: With a Case Study on the Structured Development of a System to Power a Condition Monitoring Unit." *Energy Harvesting and Systems* 1:101.

Dondi, D., A. Bertacchini, D. Brunelli, L. Larcher, and L. Benini. 2008. "Modeling and Optimization of a Solar Energy Harvester System for Self-Powered Wireless Sensor Networks." *IEEE Transactions on Industrial Electronics* 55(7):2759–66.

Gongora-Rubio, M. R., P. Espinoza-Vallejos, L. Sola-Laguna, and J. J. Santiago-Aviles. 2001. "Overview of Low Temperature Co-Fired Ceramics Tape Technology for Meso-System Technology (MsST)." *Sensors and Actuators a-Physical* 89(3):222–41.

Islam, R. A., and S. Priya. 2006. "Realization of High-Energy Density Polycrystalline Piezoelectric Ceramics." *Applied Physics Letters* 88:032903.

Kambale, R. C., J.-E. Kang, W.-H. Yoon, D.-S. Park, J.-J. Choi, C.-W. Ahn, J.-W. Kim, B.-D. Hahn, D.-Y. Jeong, Y.-D. Kim, et al. 2014. "Magneto-Mechano-Electric (MME) Energy Harvesting Properties of Piezoelectric Macro-Fiber Composite/Ni Magnetoelectric Generator." *Energy Harvesting and Systems* 1:3.

Khaligh, A., P. Zeng, and C. Zheng. 2010. "Kinetic Energy Harvesting Using Piezoelectric and Electromagnetic Technologies-State of the Art." *IEEE Transactions on Industrial Electronics* 57(3): 850–60.

Kong, N., D. S. Ha, A. Erturk, and D. J. Inman. 2010. "Resistive Impedance Matching Circuit for Piezoelectric Energy Harvesting." *Journal of Intelligent Material Systems and Structures* 21(13):1293–302.

Leonov, V., T. Torfs, P. Fiorini, and C. Van Hoof. 2007. "Thermoelectric Converters of Human Warmth for Self-Powered Wireless Sensor Nodes." *IEEE Sensors Journal* 7(5–6):650–57.

Liu, D., Y. K. Yan, and H. P. Zhou. 2007. "Synthesis of Micron-Scale Platelet $BaTiO_3$." *Journal of American Ceramic Society* 90(4):1323–26.

Messing, G. L., S. Trolier-McKinstry, E. M. Sabolsky, C. Duran, S. Kwon, B. Brahmaroutu, P. Park, H. Yilmaz, P. W. Rehrig, K. B. Eitel, et al. 2004. "Templated Grain Growth of Textured Piezoelectric Ceramics." *Critical Reviews in Solid State and Materials Sciences* 29(2):45–96.

Mitcheson, P. D., E. M. Yeatman, G. K. Rao, A. S. Holmes, and T. C. Green. 2008. "Energy Harvesting From Human and Machine Motion for Wireless Electronic Devices." *Proceedings of the IEEE* 96(9):1457–86.

Priya, S. 2010. "Criterion for Material Selection in Design of Bulk Piezoelectric Energy Harvesters." *IEEE Transactions on Ultrasonics Ferroelectrics and Frequency Control* 57(12): 2610–12.

Roundy, S., and P. K. Wright. 2004. "A Piezoelectric Vibration Based Generator for Wireless Electronics." *Smart Materials & Structures* 13(5):1131–42.

Sabolsky, E. M., G. L. Messing, and S. Trolier-McKinstry. 2001. "Kinetics of Templated Grain Growth of $0.65Pb(Mg_{1/3}Nb_{2/3})O_3$-$0.35PbTiO_3$." *Journal of the American Ceramic Society* 84(11):2507–13.

Tani, T., and T. Kimura. 2006. "Reactive-Templated Grain Growth Processing for Lead Free Piezoelectric Ceramics." *Advances in Applied Ceramics* 105(1):55–63.

Yan, Y., Y. Zhou, and S. Priya. 2014. "Enhanced Electromechanical Coupling in $Pb(Mg_{1/3}Nb_{2/3})O_3$-$PbTiO_3$<001>$_C$ Radially Textured Cylinders." *Applied Physics Letters* 104:012910.

Yan, Y. K., K. H. Cho, D. Maurya, A. Kumar, S. Kalinin, A. Khachaturyan, and S. Priya. 2013. "Giant Energy Density in<001>-Textured $Pb(Mg_{1/3}Nb_{2/3})O_3$-$PbZrO_3$-$PbTiO_3$ Piezoelectric Ceramics." *Applied Physics Letters* 102:042903.

Yan, Y. K., Y. U. Wang, and S. Priya. 2012. "Electromechanical Behavior of<001>-Textured $Pb(Mg_{1/3}Nb_{2/3})O_3$-$PbTiO_3$ Ceramics." *Applied Physics Letters* 100:192905.

Zhang, S. J., S. M. Lee, D. H. Kim, H. Y. Lee, and T. R. Shrout. 2008. "Characterization of Mn-Modified $Pb(Mg_{1/3}Nb_{2/3})O_3$-$PbZrO_3$-$PbTiO_3$ Single Crystals for High Power Broad Bandwidth Transducers." *Applied Physics Letters* 93:122908.

Zhu, D., A. Almusallam, S. P. Beeby, J. Tudor, and N. R. Harris. 2010. "A Bimorph Multi-Layer Piezoelectric Vibration Energy Harvester." Power MEMS 2010, Leuven, Belgium, December 1–3, 335–338.